Joint inversions with the SimPEG framework

Joseph Capriotti, Lindsey J. Heagy*, and Santiago Soler**
**Geophysical Inversion Facility, Department of Earth, Ocean and Atmospheric Sciences, University of British Columbia*

SUMMARY

Joint inversions seek to take advantage of the multiple geophysical surveys to produce spatially consistent results. There are many different approaches to joint inversion that all have their own characteristics. Performing a joint inversion is normally a cumbersome process that does not allow the practitioner to easily test different joint inversion methods. We have extended the open source python package SimPEG's modular framework to support several different methods of joint inversion that can be used interchangeably, notably cross-gradient, joint total variation, and petrophysically guided inversion. We use this framework to investigate gravity and magnetic joint inversion characteristics for a mining carbon mineralization project that is searching for serpentinized rock. The framework allowed for us to rapidly produce different joint inversion algorithms for each method with minimal differences between the three codes. All of the joint inversions were successful at producing strongly correlated density and susceptibility models. These unified models allow us to have a higher confidence in the interpretations.

INTRODUCTION

Different geophysical methods respond to different physical properties in manners that are dependent on the physics of those methods. When inverted separately we could then obtain inconsistent interpretations of the subsurface. Joint inversions seek to obtain physical property models that are similar to each other while still reproducing the observed geophysical data. In the most general sense, joint inversion enhances correlations between physical properties. By using multiple geophysical methods we intend to reduce uncertainty in our interpretation. Despite the attention paid to the topic in recent publications, joint inversion remains to be a difficult tool to apply in practice; not only are there many different styles of joint inversion, they also lead to complicated inversions with many choosable parameters that are difficult to determine. To these ends we've implemented a joint inversion framework within SimPEG (Cockett et al., 2015), an open source geophysical simulation and inversion python package, flexible enough to allow the user to experiment with several different forms of joint inversion.

As a motivating example for joint inversion, we will consider applying joint inversion to locating potential mining deposits for carbon mineralization. Converting atmospheric carbon dioxide (CO_2) into carbonates is an attractive option for CO_2 sequestration as the carbon is stored over geologic time scales (Lackner et al., 1995). In particular, serpentinized ultramafic rocks, which often coincide with economic minerals, have a significant sequestration potential. One mechanism for the permanent removal of CO_2 is to mine these rocks and expose them at the surface or possibly to inject CO_2 into deeper units. Identifying possible serpentinized rocks may allow for carbon neutral or even carbon negative mining operations. Serpentinized rocks have a lower density and higher magnetic susceptibility than their fresh ultramafic hosts. The carbonation process then increases the density and decreases the susceptibility (Cutts et al., 2021). Thus, geophysics is a tool of choice to efficiently assess, at a first-order, the location and volumes of serpentinized and carbonated rocks. With joint inversion, we want to better identify the serpentinized units using both gravity and magnetic surveys by their combined values of density and susceptibility. We will use a synthetic model developed in Heagy et al. (2022) that is loosely based off of the Decar site in BC, Canada (Mitchinson et al., 2020).

The joint inversion problem requires a mechanism to link the two physical properties together spatially. Joint inversions methods generally fall into two categories: the first seeks to constrain the recovered physical properties to have similar structures to each other (e.g. Haber and Oldenburg, 1997; Gallardo and Meju, 2003, 2004; Fregoso and Gallardo, 2009; Zhdanov et al., 2012; Haber and Holtzman-Gazit, 2013), and the second class encourages petrophysical relationships between the recovered physical properties (e.g. Paasche and Tronicke, 2007; Lelièvre et al., 2012; Zhdanov et al., 2012; Sun and Li, 2015; Liang et al., 2016). Structural similarity measures compare spatial gradients of models to each other to align the physical property contours. Petrophysical relationships can be predetermined through lab based measurements, or inferred through the inversion process. Within each of these classes are multiple different methods, each with their own strengths.

Ideally, we want to understand the behavior of the different methods and be able to test multiple of them on a given problem. SimPEG is a modular toolbox for geophysical inversion that allows us to develop these joint inversion strategies within a flexible framework. We have implemented three forms of joint inversion within this framework: cross-gradient (CG) of Gallardo and Meju (2003), joint total variation (JTV) from Haber and Holtzman-Gazit (2013) and petrophysically guided inversion (PGI) from Astic et al. (2021). We will apply the three different methods to our carbon mineralization example and discuss the characteristics of the solutions, as well as implementation details for the framework.

JOINT INVERSION METHODS

The joint inversion schemes that we implement all start from the Tikhonov inversion consisting of data misfit function of a data misfit, ϕ_d, and a regularization function, ϕ_m,

$$\min_{m} \phi(m) = \phi_d(m) + \beta \phi_m(m) \tag{1}$$

The regularization function measures deviations from a reference model for both the model values and their derivatives, referred to a the smallest and flattest models respectively:

$$\phi(m) = \alpha_s \int_V w_s (m - m_{ref})^2 \mathrm{d}V + \alpha_f \int_V w_f |Q \nabla (m - m_{ref})|^2 \mathrm{d}V. \tag{2}$$

Within these regularization functions, we can adjust the reference model, m_{ref}, and both cell weights, w_s and face weights, w_f to influence the recovered model. In the flattest model term, the spatial gradients may be weighted towards certain directions with the matrix Q, and the reference model may be optionally neglected. In joint inversion we have multiple data misfits, regularization functions, and generally a term to couple the models together; all of these functions are multiplied by weighting parameters and added together to form a single objective function,

$$\min_{m_1,\ldots,m_N} \phi(m_1,\ldots,m_N) = \left(\sum_{k}^{N} \phi_{d,k}(m) + \beta_k \phi_{m,k}(m) \right) + \lambda \phi_{joint}(m_1,\ldots,m_N), \tag{3}$$

for N physical property models, The coupling function, ϕ_{joint} serves to link some aspects of the physical properties together, which we will discuss further. Finally, we use a Gauss-Newton approach to minimize the non-linear joint inversions.

The structural based methods in some manner link together the spatial gradients of model parameters. The model gradients are the normals to the contours of the models, and thus these encourage similar shaped contours. The most common of these spatial gradient comparisons is the cross-gradient method of Gallardo and Meju (2004),

$$\phi_{joint} = \phi_{CG}(m_1, m_2) = \int_V |\nabla m_1 \times \nabla m_2|^2 \mathrm{d}V. \tag{4}$$

The cross product between two vectors is minimized when they're parallel to each other or when either is zero. By minimizing the cross product of model gradients, the models are encouraged to have gradients in the same direction; this enhances the similarity of the two models. Two vectors being parallel to each other, is equivalent to them being linearly related to each other. The cross-gradient measure therefore encourages linear relationships between model gradients, which subsequently encourages linear relationships between model values due to the linear gradient operator.

Joint total variation (JTV) from Haber and Holtzman-Gazit (2013) is another joint inversion measure that falls into the structural based methods. It is a measure of joint sparsity that couples the gradients of the models together by encouraging them to occur in the same spatial location. They are coupled together using the square root function,

$$\phi_{joint} = \phi_{JTV}(m_1, m_2) = \int_V \sqrt{|\nabla m_1|^2 + |\nabla m_2|^2} \mathrm{d}V. \tag{5}$$

To understand how this function encourages similarity, consider two gradients, each with a single location of non-zero magnitude, g_1 and g_2, respectively. If the gradients are non-zero in the same location, the integral evaluates to $\sqrt{g_1^2 + g_2^2}$; if they are non zero in different locations we have $|g_1| + |g_2|$. Given the triangular inequality, we know that $\sqrt{g_1^2 + g_2^2} \leq |g_1| + |g_2|$. Therefore, given two models, the JTV measure has a relatively lower penalty if both are non-zero in the same location. This method is advantageous because it is simpler than the cross-gradient method to use in minimization routines due to it being a convex function with respect to the two models m_1 and m_2. Other structural joint inversion approaches are not generally convex and can lead to difficulties in minimization routines associated with inversion.

The third method we will compare here is in the clustering based method in the petrophysical physical class of joint inversions, petrophysically guided inversions (PGI) (Astic et al., 2021). It can be summarized as iteratively updating the reference model. m_{ref}, and cell weights, w_c, of a Tikhonov regularized inversion based on the joint distribution of model parameters. It implements the smallest model regularization term as a Gaussian Mixture Model whose means are either given or learned throughout the inversion, as opposed to the assumed single Gaussians of standard Tikhonov inversions. The standard deviations of each Gaussian account for uncertainties in petrophysical data and will therefore control the tightness of clustering for each physical property. It is different from other joint inversion methods in that it is not a direct penalty term added to the minimization function. This can be applied with petrophysical information to encourage recovered model values to match the petrophysical distribution, or independent of petrophysics to encourage model values to be jointly distributed.

IMPLEMENTATION IN SIMPEG

SimPEG is developed as a modular system to implement geophysical forward simulation and gradient based inversions. The inversion process is broken down into separate pieces that can be interchanged between methods. One class handles the geophysical simulation, another class handles the regularization functions, another class performs the minimization, etc. The pieces are then assembled into an inversion.

The necessary machinery to perform a joint inversion extends beyond the standard single domain inversion. In addition to implementing the various different joint inversion methods, it requires designing an objective function that includes multiple data misfit measures, multiple regularizations functions, and the linkage objectives functions. We also need a mechanism to adjust all the individual weighting parameters to successfully perform the inversion. SimPEG's modular structure fits into these requirements.

The key class to help us enable joint inversion in SimPEG are our composable objective functions, which we can multiply by constants and add together. These objective functions have defined evaluation, derivative, and (approximate) second derivatives. Data misfit functions can be added to each other, along with regularization objective functions. An objective function is then passed to a minimization class to perform the inversion. In a joint inversion, we add together multiple data misfits, regularizations, and the coupling term to create the composite objective function that is minimized in the inversion. The minimization machinery is ambivalent to the nature of the objective function, so long as each term has methods for computing their values and derivatives given a model. The open source nature of the project also allows others to contribute their own implementations, and the CG regularization function was originally contributed by Wei and Sun (2021).

The next key aspect to the joint inversion is choosing and updating all of the hyperparameters that control the weight of each component of the objective function. SimPEG controls these parameters through directives, which describe conditions to update them throughout the inversion iterations. These directives can update cell weights, adjust weighting parameters, change regularization functions, etc.

We have designed a set of directives to handle the joint inversion problem. The CG and JTV methods required a directive to ensure that each data misfit reaches the prescribed level by iteratively adjusting their weighting parameters. The PGI directives adjust the cell weights and reference model at each iteration to perform the joint inversion.

APPLICATION TO CARBON MINERALIZATION

We apply this joint inversion framework to a simplified synthetic carbon mineralization test problem. Our goal is to compare the character of the solutions to the different joint inversion methods to learn more about their behavior for this type of problem. The synthetic model, Figure 1, consists of a single unit with a carbonated zone between two serpentinized zones. The background has 2.9 g/cc density and 0 SI susceptibility, the carbonated rock has 3.0 g/cc density and 0.05 SI susceptibility, and the serpentinized rock has 2.7 g/cc density and 0.15 SI susceptibility. We simulate a surface gravity survey and an airborne total magnetic anomaly magnetic survey on a 19 km by 21 km area with 250 m grid spacing in x and y. The magnetic survey has a vertical inducing field. We have added unbiased Gaussian noise with standard deviation of 0.01 mGal and 1 nT, respectively, to the simulated data.

To compare against the joint inversion results, we performed separate Tikhnov inversions measuring ℓ_2 norms, with the density and susceptibility models shown in Figure 2. The cross-plot shows little correlation between density and susceptibility. The two models agree with the horizontal location of the anomalies, but the depths and overall shapes are not consistent.

The CG results, Figure 3, show two distinct linear relationships between density and susceptibility between the three units in the model, one between the background and the serpentinized unit, and a second from the serpentinized unit to the carbonated unit. The cross-plot in Figure 3 shows the density and susceptibility pair in each model cell, each point is plotted with a transparency, and where many points overlap, the plot will be darker. This gives us a first order intuition of the petro-

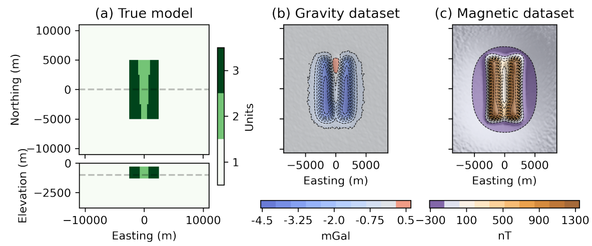

Figure 1: (a) The simplified carbon mineralization model. The serpentinized unit, unit 3, has a density of 2.7 g/cc, and 0.15 SI susceptibility and the carbonated unit, unit 2, has a density of 3.0 g/cc and 0.05 SI susceptibility, relative to the background, unit 1, with 2.9 g/cc density and 0 susceptibility. We simulate a gravity (b) and magnetic survey (c) on a 19 km by 21 km grid with 250 m grid spacing.

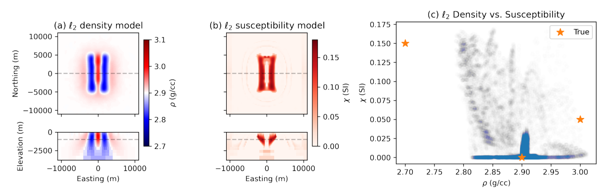

Figure 2: The cross-plot of recovered density and susceptibility values from separate ℓ_2 single domain inversions. The cross-plot shows little correlation between the physical properties.

physical probability density function of the model parameters. The linear transitions between units are due to the spatial location of the three units in the resultant model; the carbonate unit is completely enclosed by the "U" shaped serpentinized unit, separating the carbonated unit from the background. One thing to note is that the cross gradient inversion also allows for structure in one model at locations where the other model is constant. To the outside of the negative density region, there are positive lobes that do not correspond to any structure in the susceptibility model. In the cross-plot, these are represented as vertical and horizontal lines at the background density and susceptibility.

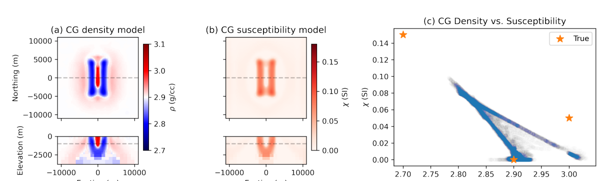

Figure 3: Recovered (a) density and (b) susceptibility models from CG inversion. (c) The physical property cross-plot shows stereotypical linear relationships between density and susceptibility due to cross gradient joint inversion.

The JTV result, Figure 3, is more compact than the CG model, due to the regularization operation encouraging sparseness on the model gradients. There are few model cells where only one physical property is non-zero. The regularization encourages the non-zeros of the spatial gradients to occur in the same physical location, which we can see by both models having non-zeros in the same locations. This creates three clusters of units which are evident in the cross-plot of model parameters, one near the background, one for the serpentinized unit, and another for the carbonated unit. The units are well located horizontally, but they extend up to the surface.

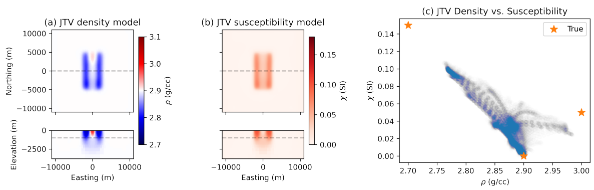

Figure 4: Recovered (a) density and (b) susceptibility models from JTV. This joint inversion has recovered more compact anomalies closer to the surface than the cross gradient approach. (c) This cross-plot shows the more clustered behavior of the physical properties due to the joint sparsity constraint on the gradient encouraging non-zeros to occur in the same spatial locations.

The PGI result shows three distinctly separate units in the petrophysical cross-plot. The density values are well clustered, however the susceptibility values are not as well clustered indicated by the broad spread of the susceptibility values within each cluster. The PGI method required a larger standard deviation in susceptibility petrophysical values for this example to properly fit the observed magnetic data. There is still good separation between the three clusters, though mostly due to density. The separation between clusters implies that the PGI method recovered sharper boundaries between units than either the CG or the JTV method.

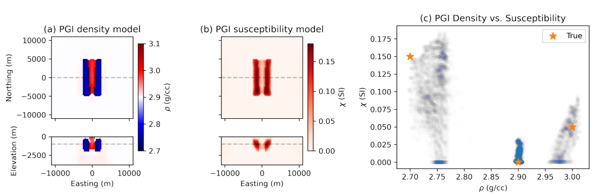

Figure 5: Recovered (a) density and (b) susceptibility models from PGI. The clustering based inversion recovered three distinctly separate units. (c) We observe three separate clusters of density and susceptibility on the cross-plot.

A next step in making interpretations from these models would be to build a quasi-geology model from the inverted results. Considering the strong correlations between physical properties in joint inversions, it can be easier to distinguish separate units in joint inversions than searching for correlations in separate single domain inversions, Figure 2. The separate ℓ_2 inversions produce models that have little structure in common with each other. PGI, since it is a clustering-based method, naturally classifies the method into separate units. Post inversion clustering methods could be more successfully applied to the JTV results than the CG results due to its more compact anomalies, and sharper transitions. CG performs closer to a standard regularized inversion with broad transitions between units. In these cases a simple method could be to estimate cutoffs from an analogous inversion, as was done in Heagy et al. (2022).

CONCLUSIONS

The appeal of joint inversion is to create consistent models of the earth from multiple geophysical surveys; separate inversions can create competing models. We can see that all of the joint inversions were successful at recovering density and susceptibility models that were visually similar to each other and showed strong correlations between physical properties. These spatially consistent models give strength to an interpretation.

The modular SimPEG framework allowed us to implement several different methods of joint inversion. We have shown how each method will behave in the carbon mineralization example. The CG method will tend to create linear relationships between physically adjacent units, the JTV will try to create compact units that are in the same location, and PGI will impose clustering on the physical properties. The modular framework, which encourages experimentation and exploration, allowed us to quickly apply all of the methods using a common structure.

The SimPEG environment and its ecosystem are designed to make it easier to build upon the current achievements and to let others contribute their ideas and software advancements. To this end, we will continue to iterate and improve these implementations. We will experiment with combining other geophysical data within the framework. There is room to implement more joint inversion strategies in this framework, and we welcome participation from others in the project.

ACKNOWLEDGMENTS

We would like to acknowledge Mitacs and Mira Geoscience for providing funding for this work through the Accelerate program. We also thank the many developers of and contributors to the SimPEG project.

REFERENCES

Astic, T., L. J. Heagy, D. W. Oldenburg, 2021, Petrophysically and geologically guided multi-physics inversion using a dynamic Gaussian mixture model: Geophysical Journal International, **224**, 40–68, doi: https://doi.org/10.1093/gji/ggaa378.

Cockett, R., S. Kang, L. J. Heagy, A. Pidlisecky, and D. W. Oldenburg, 2015, SimPEG: An open source framework for simulation and gradient based parameter estimation in geophysical applications: Computers & Geosciences, **85**, 142–154, doi: https://doi.org/10.1016/j.cageo.2015.09.015.

Cutts, J. A., K. Steinthorsdottir, C. Turvey, G. Dipple, R. J. Enkin, and S. M. Peacock, 2021, Deducing mineralogy of serpentinized and carbonated ultramafic rocks using physical properties with implications for carbon sequestration and subduction zone dynamics: Geochemistry, Geophysics, Geosystems, **22**, e2021GC009989, doi: https://doi.org/10.1029/2021GC009989.

Fregoso, E., and L. A. Gallardo, 2009, Cross-gradients joint 3d inversion with applications to gravity and magnetic data: Geophysics, **74**, no. 4, L31–L42, doi: https://doi.org/10.1190/1.3119263.

Gallardo, L. A., and M. A. Meju, 2003, Characterization of heterogeneous near-surface materials by joint 2D inversion of dc resistivity and seismic data: Geophysical Research Letters, **30**, 1658, doi: https://doi.org/10.1029/2003GL017370

Gallardo, L. A., and M. A. Meju, 2004, Joint two-dimensional dc resistivity and seismic travel time inversion with cross-gradients constraints: Journal of Geophysical Research: Solid Earth, **109**, 3311, doi: https://doi.org/10.1029/2003JB002716.

Haber, E., and M. Holtzman-Gazit, 2013, Model fusion and joint inversion: Surveys in Geophysics, **34**, 675–695, doi: https://doi.org/10.1007/s10712-013-9232-4.

Haber, E., and D. Oldenburg, 1997, Joint inversion: a structural approach: Inverse Problems, **13**, 63, doi: https://doi.org/10.1088/0266-5611/13/1/006.

Heagy, L., T. Astic, J. Capriotti, J. Weis, and D. Oldenburg, 2022, Geophysical inversions to delineate rocks with CO2 sequestration potential through carbon mineralization: FastTIMES, **26**, 4, doi: https://doi.org/10.48550/arXiv.2203.13894.

Lackner, K. S., C. H. Wendt, D. P. Butt, E. L. Joyce Jr, and D. H. Sharp, 1995, Carbon dioxide disposal in carbonate minerals: Energy, **20**, 1153–1170, doi: https://doi.org/10.1016/0360-5442(95)00071-N.

Lelièvre, P. G., C. G. Farquharson, and C. A. Hurich, 2012, Joint inversion of seismic traveltimes and gravity data on unstructured grids with application to mineral exploration: Geophysics, **77**, K1–K15, doi: https://doi.org/10.1190/geo2011-0154.1.

Liang, L., A. Abubakar, and T. M. Habashy, 2016, Reservoir property mapping and monitoring from joint inversion of time-lapse seismic, electromagnetic, and production data: Geophysics, **81**, no. 5, ID73–ID84, doi: https://doi.org/10.1190/geo2015-0620.1.

Mitchinson, D., J. Cutts, D. Fournier, A. Naylor, G. Dipple, C. Hart, C. Turvey, M. Rahimi, and D. Milidragovic, 2020, The carbon mineralization potential of ultramafic rocks in British Columbia: a preliminary assessment: Technical Report Geoscience BC Report 2020-15, MDRU Publication, 452.

Paasche, H., and J. Tronicke, 2007, Cooperative inversion of 2D geophysical data sets: A zonal approach based on fuzzy c-means cluster analysis: Geophysics, **72**, no. 3, A35–A39, doi: https://doi.org/10.1190/1.2670341.

Sun, J., and Y. Li, 2015, Multidomain petrophysically constrained inversion and geology differentiation using guided fuzzy c-means clustering: Geophysics, **80**, no. 4, ID1–ID18, doi: https://doi.org/10.1190/geo2014-0049.1.

Wei, X., and J. Sun, 2021, 3D probabilistic geology differentiation based on airborne geophysics, mixed LP norm joint inversion and petrophysical measurements: Earth and Space Science Open Archive, **12**, 762, doi: https://doi.org/10.1002/essoar.10508762.1.

Zhdanov, M. S., A. Gribenko, and G. Wilson, 2012, Generalized joint inversion of multimodal geophysical data using Gramian constraints: Geophysical Research Letters, **39**, 9301, doi: https://doi.org/10.1029/2012GL051233.